



Crashworthiness of Energy Absorbing Structures Under Combined Shear-Compression Loading: Effects of Materials and Geometries

Yong-Ha Hwang¹ · Jae-Hung Han¹

Received: 17 March 2024 / Revised: 26 May 2024 / Accepted: 22 June 2024
© The Author(s) 2024

Abstract

In this paper, a study on the design of energy absorbing structures under combined shear-compression loading is conducted to effectively utilize the energy absorption principles of the material. Concave and convex designs are applied to energy absorbing structures made of metallic and braided composite materials. The energy absorption principles vary depending on the characteristics of each material. For metal, a design maximizing energy absorption through plastic deformation is necessary. Concave and convex designs induce initial crushing due to stress concentration under loads, reducing the maximum load. Subsequently, the load is distributed throughout the entire structure, improving load-bearing performance and enhancing energy absorption performance. Braided composites demonstrate superior characteristics in terms of specific stiffness, specific strength, and specific energy absorption when compared to metals. They absorb energy through damage accumulation in the laminate. Therefore, to optimize the performance, inducing a progressive failure mode becomes necessary. Unlike metals, braided composites can achieve effective energy absorption performance without altering the geometric shape. Energy absorbing structures are manufactured, and drop impact tests are carried out to assess their performance. In conclusion, it is observed that the geometric shapes effective in enhancing crashworthiness performance vary according to the energy absorption principles of each material. Also, the energy absorption per unit volume is found to be superior for metal energy absorbing structures, whereas the energy absorption per unit mass is better for composite energy absorbing structures. Therefore, depending on the application, both metals and composites can be effectively utilized as materials for energy absorbing structures.

Keywords Combined shear-compression loading · Crashworthiness · Drop impact test · Metallic material · Braided composite

1 Introduction

Crashworthiness is defined as the ability of a vehicle to protect its occupants from injury in the event of a crash [1]. As technology advances, our reliance on vehicles has increased, resulting in more vehicles on the roads and faster transportation. It means that the possibility of catastrophic accidents caused by vehicle collision has increased compared to the past. Accordingly, the importance of crashworthiness to protect passengers and payloads is also increasing [2].

Energy absorbing structures, as a type of passive protection system, are designed to convert kinetic energy from

collisions into other forms of energy, thereby reducing the damage transmitted to passengers and payloads [3]. Metallic cylindrical shells are commonly used as energy absorbing structures in various applications [4, 5], such as longitudinal frames of automobiles and front structures of trains [6]. When a force is applied, the metallic energy absorbing structure dissipates kinetic energy by deforming plastically. The key to effective energy absorption is to promote progressive crushing of the metallic energy absorbing structure, which maximizes the amount of kinetic energy that can be absorbed. If the energy absorbing structure bends globally, its ability to absorb energy decreases, which compromises passenger safety.

Because of its high strength-to-weight ratio [7], composites are also gaining attention for energy absorbing structures and can be applied to various applications [8–10]. The composite braiding technique is used to produce a composite

Communicated by JAE-SANG PARK.

✉ Jae-Hung Han
jaehunghan@kaist.ac.kr

¹ Department of Aerospace Engineering, KAIST, 291
Daehak-Ro, Yuseong-Gu, Daejeon 34141, Republic of Korea

part by intertwining fibers to create a desired braid architecture before or during the impregnation of the fibers. Braided composite shows stable impact resistance, which is benefited from the interweaving of the fibers [11]. There are various studies aimed at assessing the crashworthiness of structures made of braided composites. Wu et al. [12] experimentally discovered that the crushing mode varies depending on the number of axial yarns. Regardless of the number of axial yarns, the most superior energy absorption performance was observed when a progressive crushing mode was induced. The same research group conducted a study on performance based on braiding angle [13]. Similarly, the induction of a progressive crushing mode had a significant impact on energy absorption performance. When the braiding angle is 60 degrees, it induces a progressive crushing mode, which is efficient for energy absorption performance. However, when the braiding angle is 45 degrees, folding occurs in the middle, making energy absorption relatively inefficient. Other research teams investigating the relationship between braid angle and energy absorption performance showed different results. Gui et al. [14] performed a quasi-static compression test. They confirmed that those with a 45-degree braid angle exhibited the highest SEA. On the contrary, Nazrul Roslan et al. [15] observed the progressive crushing mode of tubes with braid angles of 30 degrees and 45 degrees, confirming the highest SEA performance in tubes with a 30-degree braid angle. Through previous research findings [13–15], it was noted that the most efficient braid angle for energy absorption may vary depending on factors such as braid architecture and tube geometry.

Unlike metallic energy absorbing structures [16], there is a lack of understanding on the crashworthiness performance of braided composites subjected to the combined shear-compression loading based on geometries. Additionally, there is a scarcity of comparative studies between metallic material and braided composites for the same geometry. Therefore, this paper aims to analyze geometries that effectively utilize the energy absorption principles of metallic materials and braided composites when subjected to the combined shear-compression loading.

2 Experimental Setup

2.1 Crashworthiness Indicators

To enhance the crashworthiness performance of energy absorbing structures, it is necessary to identify the characteristics that ideal energy absorbing structures should possess. Lu et al. [2] summarized the characteristics of ideal energy absorbing structures as follows.

- The energy conversion should be irreversible.

- The peak force should be restricted and the reaction force should be constant.
- Stable and repeatable deformation mode while ensuring a long stroke.
- Light weight, high specific energy absorption capacity.

Based on the characteristics of an ideal energy absorbing structures, the most commonly used quantitative indicators for evaluating the performance of energy absorbing structures are specific energy absorption (SEA) and crush force efficiency (CFE). The specific energy absorption (SEA) is determined by dividing the energy absorption (E_a) by the mass of the energy absorbing structure (m). E_a is defined as the area under the force–displacement curve. Crush force efficiency (CFE), indicative of load uniformity, is derived by dividing the mean crushing force (F_m) by the peak force (F_{max}) from the force–displacement curve. F_m is calculated as the ratio of E_a to the crushing length (δ). Expressions for SEA, CFE, and F_m are provided in Eqs. (1) through (3). The performance of metallic energy absorbing structures is compared with that of braided energy absorbing structures. To facilitate the performance comparison, the energy absorption per volume of the energy absorbing structure is defined in Eq. (4) [17]. Thus, in this paper, SEA, CFE and E_v are used as indicators of crashworthiness performance [17–19].

$$SEA = \frac{\int_0^{\delta} F(x)dx}{m} = \frac{E_a}{m}, \quad (1)$$

$$CFE = \frac{F_m}{F_{max}}, \quad (2)$$

$$F_m = \frac{E_a}{\delta}, \quad (3)$$

$$E_v = \frac{E_a}{V} \quad (V = \text{Volume of the energy absorbing structure}). \quad (4)$$

2.2 Specimen Manufacturing

Ductile metals and composites are representative isotropic and anisotropic materials, respectively. As depicted in Fig. 1, the different energy absorption principles of ductile metals and composites result in inducing different crushing modes for the same geometry. For ductile metal, a design maximizing plastic deformation should be implemented to effectively utilize its high ductility. In the case of composite materials, it is possible to achieve a higher specific stiffness, specific strength, and specific energy absorption compared to ductile metals. Additionally, predominantly brittle failure occurs due to the lower ductility. As a result, the energy absorption principles differ, and to maximize energy absorption, the

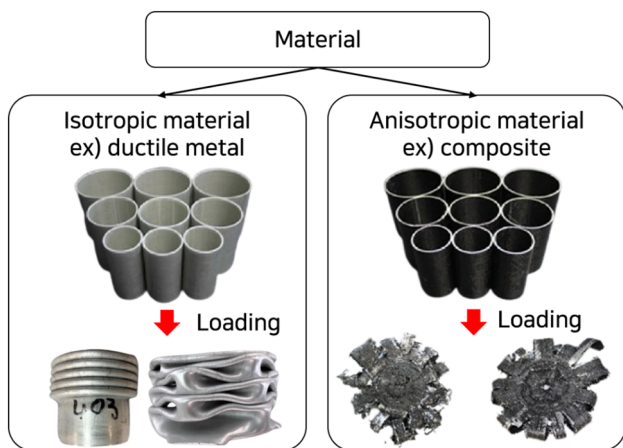


Fig. 1 Classification of materials for energy absorbing structures [20–22]: Ductile metal, composite

Table 1 Mechanical properties of the EGI [23]

| | |
|------------------|---------|
| Young’s modulus | 200GPa |
| Poisson’s ratio | 0.3 |
| Yield strength | 215 MPa |
| Tensile strength | 332 MPa |
| Elongation | 42% |

accumulation of damage in the laminate must be maximized. Therefore, to maximize the performance of composite energy absorbing structures, inducing a progressive crushing mode is essential. Electro-galvanized iron (EGI) is a type of steel renowned for its outstanding ductility. In this paper, EGI and a braided composite were utilized as materials for the energy absorbing structure. The properties of EGI and the braided composite are presented in Table 1 and Table 2.

Figure 2a illustrates the manufacturing process of an energy absorbing structures, utilizing sheet metal. After rolling two sheet metals, they are welded to create concave and convex designs. Figure 2b shows the manufacturing process of an energy absorbing structure using braiding techniques. A cylindrical mandrel and a mold were manufactured. Subsequently, braiding yarns (T700), released from the yarn spindles, were arranged in a staggered pattern at a 45-degree angle in the helical direction, forming a single ply. The diameter of the carbon fibers utilized in this paper is approximately 7 μm (0.007mm). Additionally, the width and thickness of the yarn composed of carbon fibers are 4mm and 0.5mm, respectively. To enhance strength for the axial loading, 16 fibers were inserted in the axial direction. Regardless of the material, the energy absorbing structure had a length of 40

Table 2 Mechanical properties of the composite laminate [8]

| Material properties | Variable | Value |
|-----------------------------------|----------------------------|-------------------------|
| Longitudinal modulus | E_{11} | 113.0 GPa |
| Transverse modulus | $E_{22} = E_{33}$ | 34.8 GPa |
| Principal Poisson’s ratio | ν_{12} | 0.07 |
| Shear modulus | $G_{12} = G_{23} = G_{13}$ | 4.9 GPa |
| Longitudinal tensile strength | X_T | 1808.0 MPa |
| Longitudinal compressive strength | X_C | 1175.2 MPa |
| Transverse tensile strength | Y_T | 563.2 MPa |
| Transverse compressive strength | Y_C | 700.0 MPa |
| In-plane shear strength | X_S | 220.0 MPa |
| Density | ρ | 1,560 kg/m ³ |

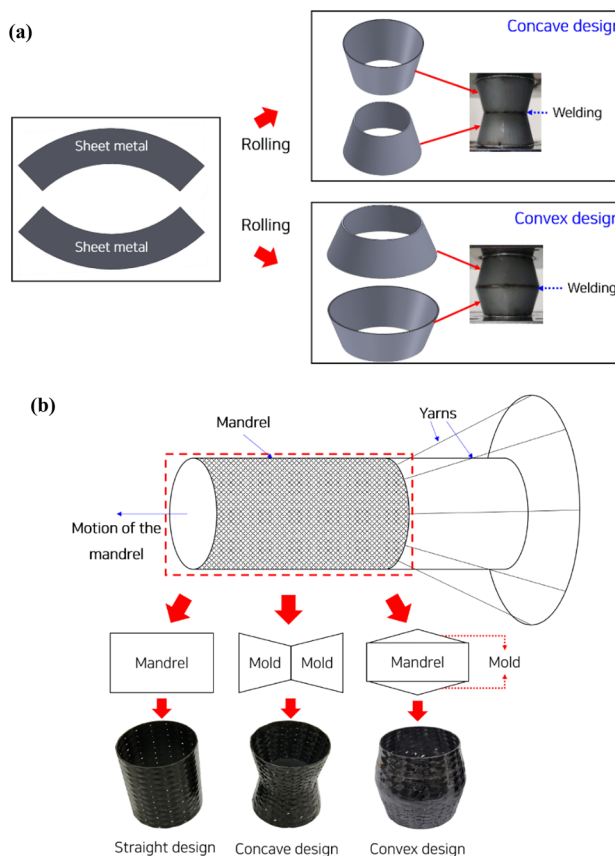


Fig. 2 Manufacturing process of specimens: a Metallic material (EGI), b Braided composite

mm and a thickness of 0.5 mm. The end diameter was 38.2 mm, while the diameters at the center of the concave and convex designs were 28.2 mm and 48.2 mm, respectively.

2.3 Drop Impact Test Setup

The drop impact test is one of the commonly used experimental methods to assess the crashworthiness performance of energy absorbing structures [2, 24], which is subjected to low-velocity impact. As shown in Fig. 3a, a drop weight was designed to weigh approximately 40kg and, once lifted by a spring balancer, it would be released by momentarily removing a pin that connected its top and bottom parts. This would cause the drop weight to fall onto the anvil plate, where the energy absorbing structure is located. The distance between the drop weight and the energy absorbing structure was approximately 0.9m. A dynamic force sensor was installed on the lower part of the energy absorbing structure to measure the instantaneous load generated during the collision between the drop weight and the energy absorbing structure. For the dynamic force sensor, the Kistler 9333A model was utilized. Additionally, the Kistler 5165A4KH11 model from the same company was used for data acquisition (DAQ). To prevent direct impact on the dynamic force sensor, 30mm thick plates were attached to its top and bottom parts. A high-speed camera, provided by Kron Technologies, was employed to record the crushing process when the drop impact occurred. Lighting plays a crucial role when using a high-speed camera. High-speed cameras are utilized to capture fast movements within very short durations, and adequate lighting is essential for their operation. Lighting

provides illumination to clearly visualize the subject and capture detailed movements or changes. It was assumed that the velocity of the drop weight decreased linearly from the moment of impact until reaching the maximum crushing length. The sampling rate of the dynamic force sensor was set at 10 kHz, while the frame rate of the high-speed camera was set at 2.5 kHz.

As depicted in Fig. 3b, a slope was manufactured to conduct a combined shear-compression loading test. The slope was linked to the bottom of the drop weight and the base of the energy absorbing structure. The drop weight descended parallel to the steel plate located to the top of the energy absorbing structure. For the energy absorbing structures fabricated with EGI, steel plates were welded to both ends. In the case of the braided composite, grooves were designed on the steel plate to prevent slippage of the energy absorbing structure. The tests were conducted at 0-degree and 30-degree angles. According to the analysis of U.S. Army helicopter accidents, it is known that 80% of survivable accidents occurred within a roll range of $\pm 20^\circ$. Based on this, the maximum load angle for the tests conducted in this paper was set to 30° . In the case of crashworthiness performance, calculations were based on the reaction force-crushing length curve when a displacement of 70% (28 mm) of the initial height of the energy absorption structure occurred [25].

3 Drop Impact Test

3.1 Metallic Energy Absorbing Structures with Straight Design

Figure 4a and b illustrates the reaction force-crushing length curve, revealing excellent test result repeatability. In the case of the straight design due to the structural characteristics without reflecting geometric imperfections, it can be observed that the initial crushing force reached the highest load on the reaction force-crushing length curve. With an increase in the loading angle, the initial crushing force remained at a high level, while the mean crushing force decreased, indicating a reduction in energy absorption performance. Figure 4c and d illustrates the crushing process. When subjected to the axial loading, it can be observed that a progressive crushing mode was induced from the bottom of the energy absorbing structure. It indicates effective utilization of the load-bearing capacity of the energy absorbing structure. On the other hand, when subjected to the combined shear-compression loading, initial crushing occurred throughout the entire structure, resulting in a decrease in overall stiffness and an inefficient utilization of load-bearing capacity.

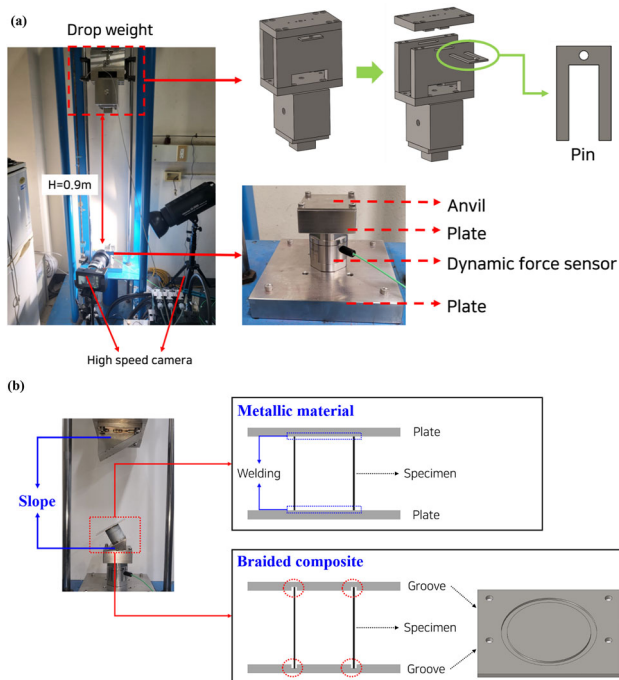


Fig. 3 Drop impact test setup: **a** Test equipment, **b** Specimen

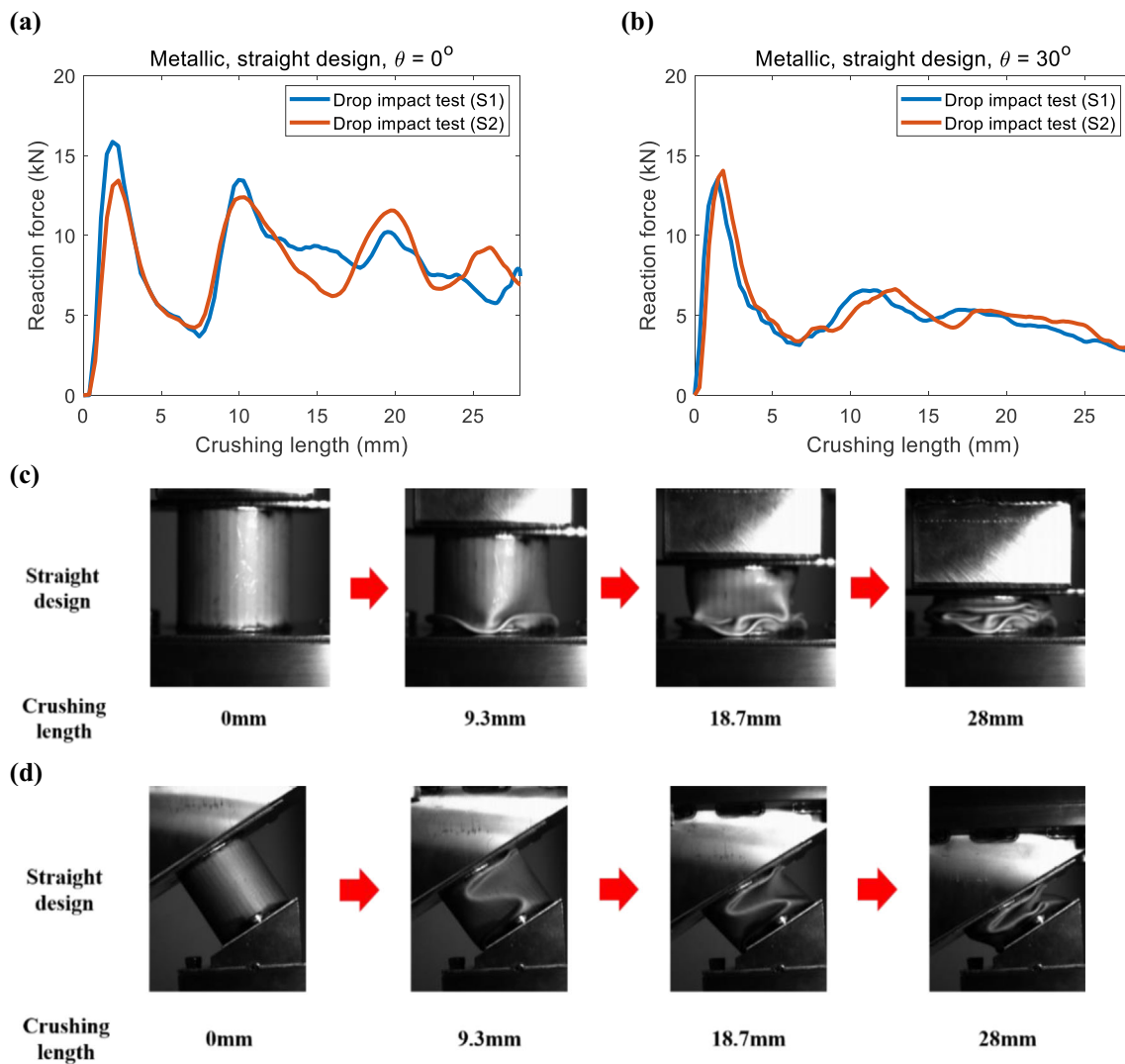


Fig. 4 A metallic, straight energy absorbing structure under low-velocity impact loading: reaction force-crushing length curve, **a** $\theta = 0^\circ$, **b** $\theta = 30^\circ$; crushing process, **c** $\theta = 0^\circ$, **d** $\theta = 30^\circ$

3.2 Metallic Energy Absorbing Structures with Concave Design

A drop impact test was performed on the concave design. High test repeatability can be confirmed through the reaction force-crushing length curve in Fig. 5a and b. It can also be confirmed that the initial crushing force was lowered due to the geometric imperfection of the concave design. Through the crushing process in Fig. 5c and d, it can be seen that regardless of the load angle, initial crushing was induced in the central part because of stress concentration, and the load was distributed to the upper and lower parts, showing high load-bearing performance.

3.3 Metallic Energy Absorbing Structures with Convex Design

The convex design shares very similar structural characteristics with the concave design. In other words, due to stress concentration at the center, the initial crushing load decreased, while the stiffness of the remaining structural areas was relatively well maintained after initial crushing, allowing for effective utilization of load-bearing capacity. This characteristic holds true regardless of the loading angle. A uniform load distribution can be observed through Fig. 6a and b. Additionally, the crushing process of the convex design under the axial loading and the combined shear-compression loading conditions can be examined through Fig. 6 (c) and (d).

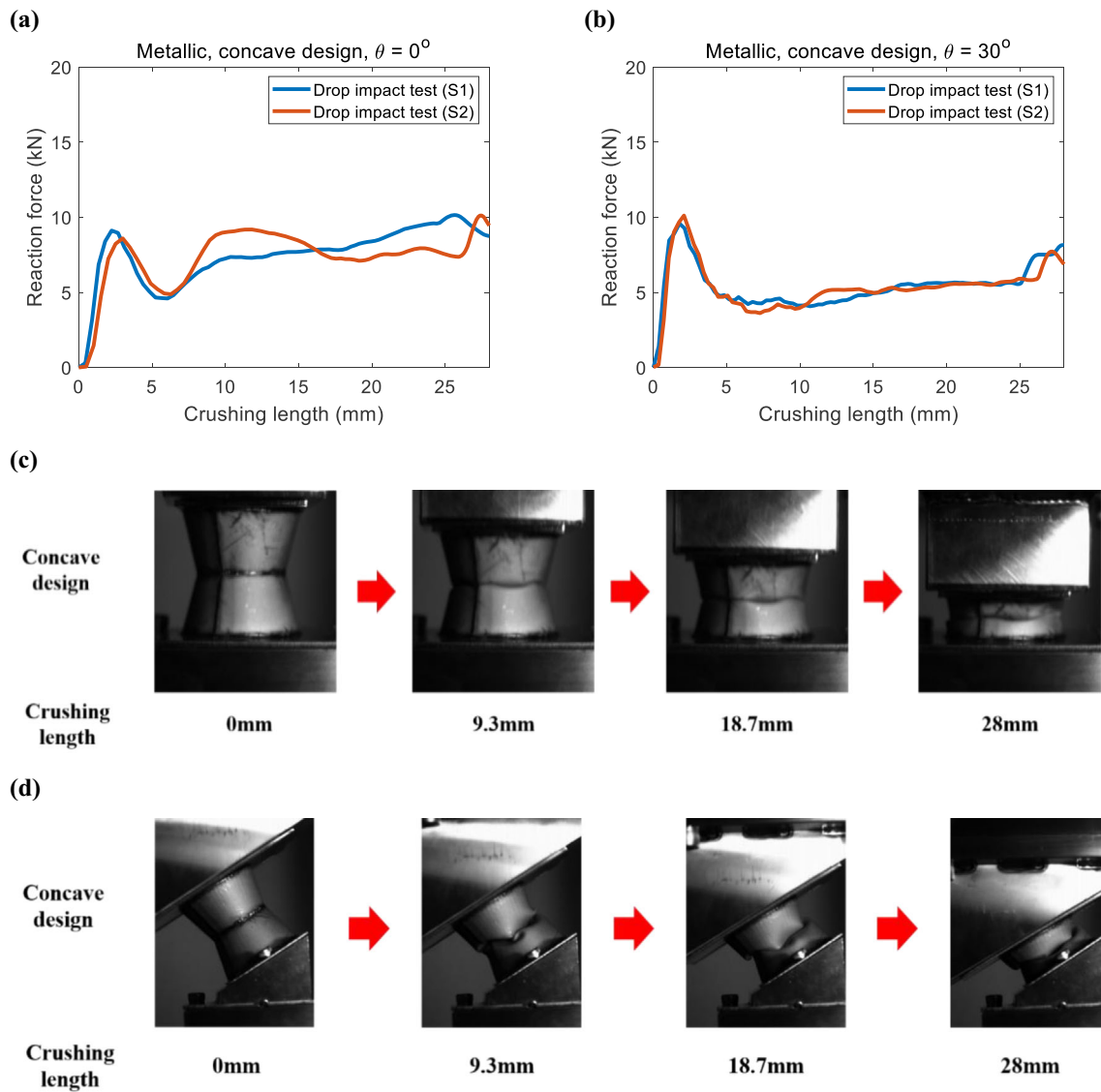


Fig. 5 A metallic, concave energy absorbing structure under low-velocity impact loading: reaction force-crushing length curve, **a** $\theta = 0^\circ$, **b** $\theta = 30^\circ$; crushing process, **c** $\theta = 0^\circ$, **d** $\theta = 30^\circ$

3.4 Braided Composite Energy Absorbing Structures with Straight Design

A drop impact test was conducted on a braided composite energy absorbing structure with a straight design. Figure 7a and b shows the reaction force-crushing length curve according to the loading angle. The consistent shape of the reaction force-crushing length curve and the high repeatability of performance metrics were confirmed. Compared to the axial loading, it can be observed that the load-bearing performance for the combined shear-compression loading was somewhat reduced. This was due to the simultaneous occurrence

of the bending mode. The bending mode weakened the load-bearing performance, resulting in a decrease in SEA performance. Figure 7c and d illustrates the crushing process with respect to the loading angle. For the axial loading, it can be observed that after initial crushing occurred at the top, a progressive crushing mode was induced, maximizing energy absorption efficiency. Also, for a 30° combined shear-compression loading, initial crushing occurred at the top. However, the bending moment occurred due to the impact load, leading to the simultaneous occurrence of the bending mode.

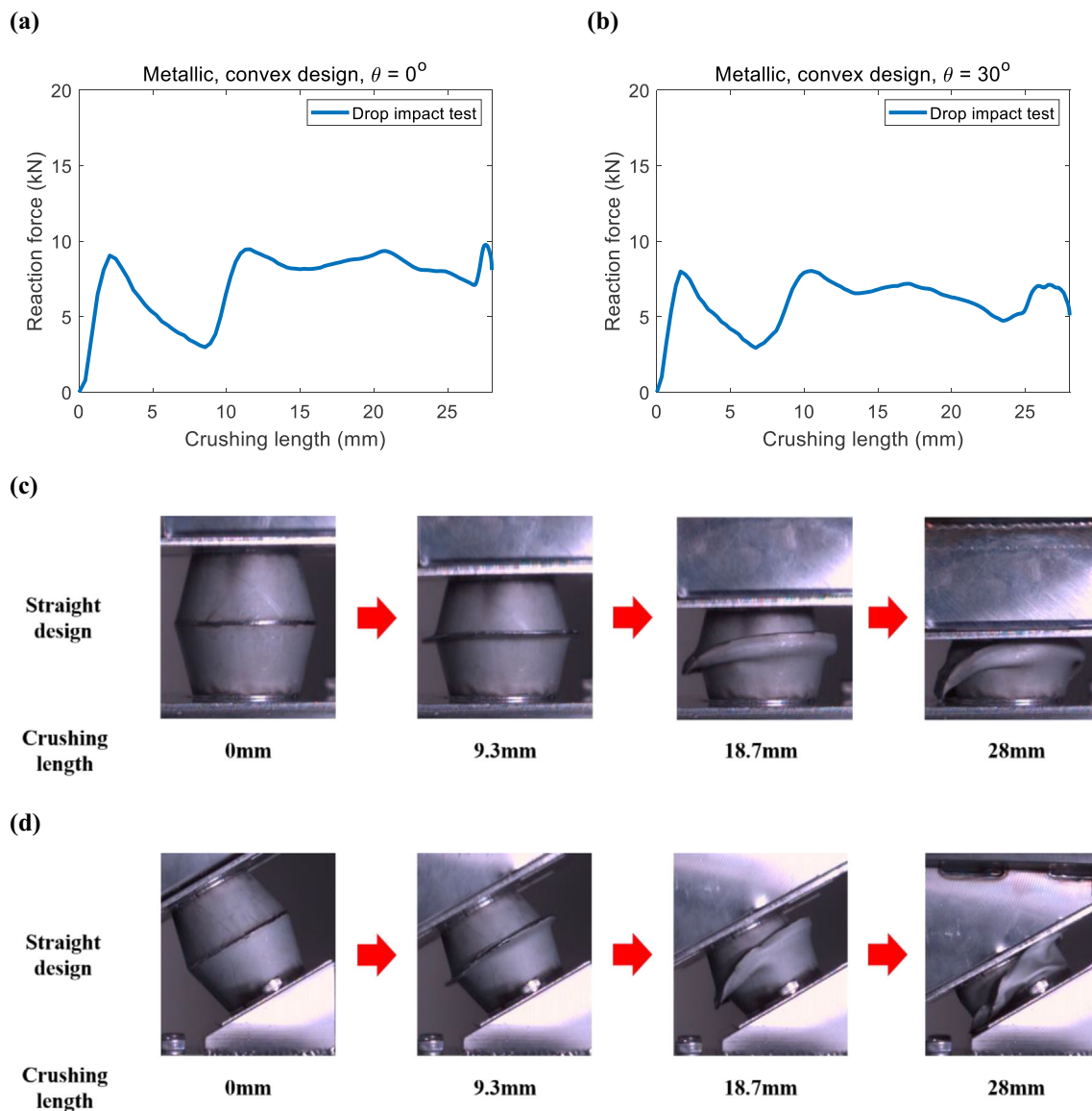


Fig. 6 A metallic, convex energy absorbing structure under low-velocity impact loading: reaction force-crushing length curve, **a** $\theta = 0^\circ$, **b** $\theta = 30^\circ$; crushing process, **c** $\theta = 0^\circ$, **d** $\theta = 30^\circ$

3.5 Braided Composite Energy Absorbing Structures with Concave Design

When a load is imposed on a braided composite energy absorbing structure with concave design, the braid material undergoes deformation. In cases where gaps exist between the fiber bundles, and the matrix material is either damaged or excessively soft, the fiber bundles can rotate freely until they become jammed against each other, as illustrated in Fig. 8. When a load is continuously applied even after jamming, interference occurs between adjacent fiber bundles. This leads to the development of cracks in the fiber bundles.

This is a factor that impairs the load-bearing performance of the energy absorption structure.

By examining the reaction force-crushing length curve in Fig. 9a, differences in the axial loading trend become apparent. In comparison to the axial loading, the combined shear-compression loading exhibits a similar trend, as illustrated in Fig. 9b.

In Fig. 9c, the crushing process of the first specimen (S1) subjected to the axial loading is observed. Initial crushing occurred in the central region where the load-bearing performance was weakened due to the bending of fibers, and the load-bearing performance was further diminished by the occurrence of cracks because of interaction between adjacent

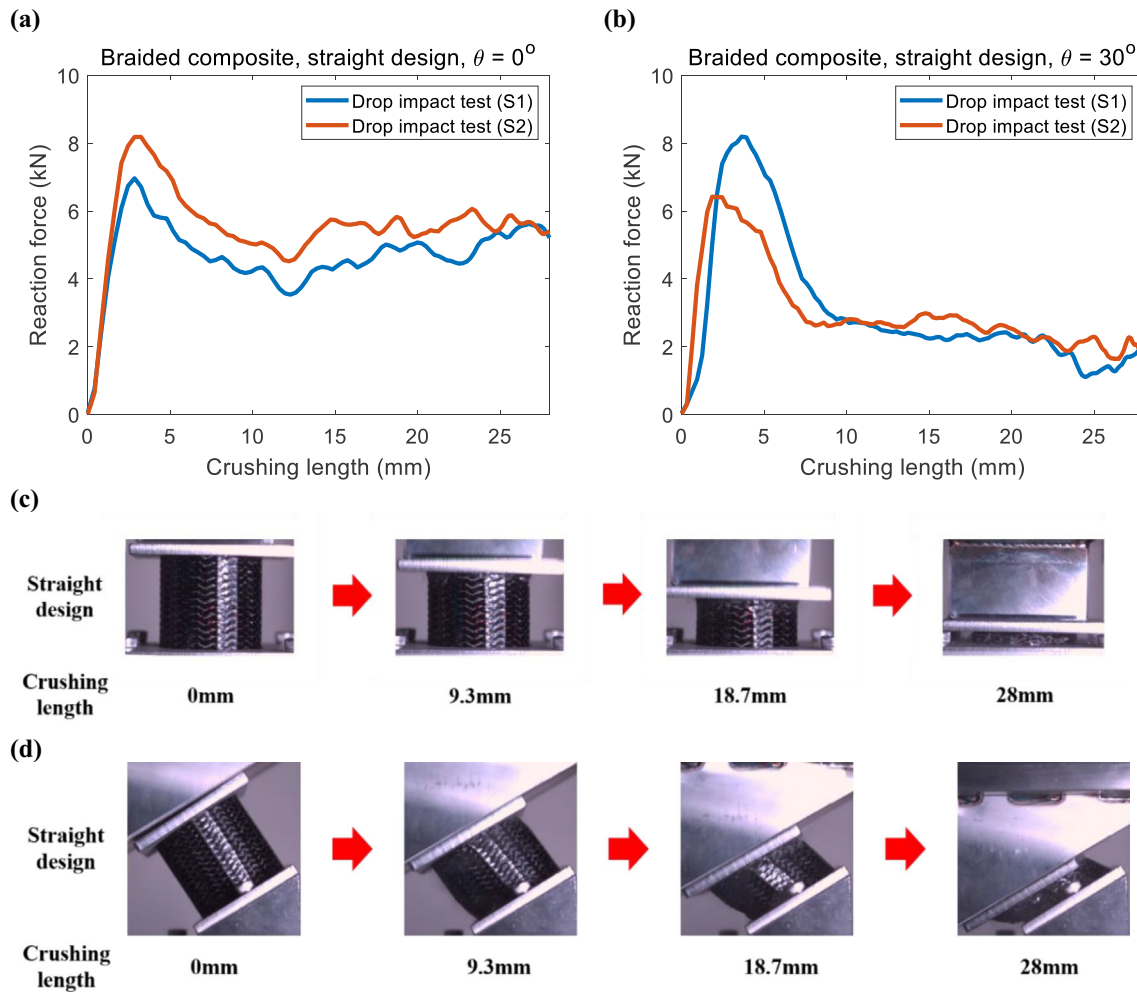
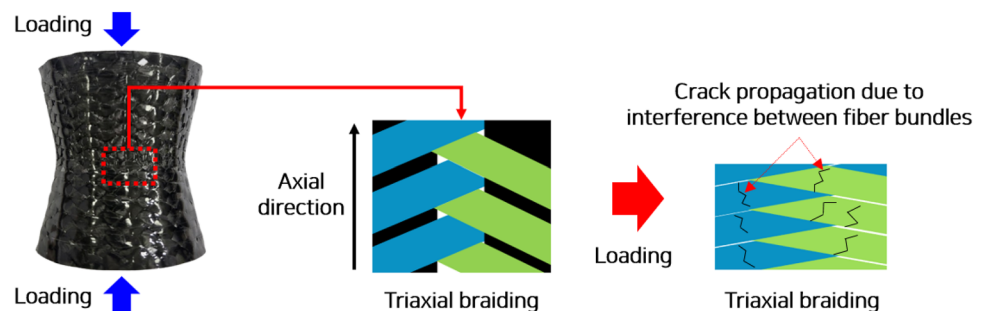


Fig. 7 A braided composite, straight energy absorbing structure under low-velocity impact loading: reaction force-crushing length curve, (a) $\theta = 0^\circ$, (b) $\theta = 30^\circ$; crushing process, (c) $\theta = 0^\circ$, (d) $\theta = 30^\circ$

Fig. 8 The crack propagation process in an energy absorbing structure with a concave design



fiber bundles. This led to a deterioration in energy absorption performance.

In Fig. 9d, the crushing process of the second specimen (S2) subjected to the axial loading is observed. The crushing process in Fig. 9d differs from that in Fig. 9c. Specifically, a progressive crushing mode was initiated from the upper portion where the impact was applied, rather than from the

central region. It demonstrates a more uniform and higher load distribution compared to the first specimen (S1).

In Fig. 9e, at an angle of 30° , damage was initiated from the central region. As the load was applied, cracks occurred, further compromising the load-bearing performance. This resulted in a deterioration of energy absorption performance.

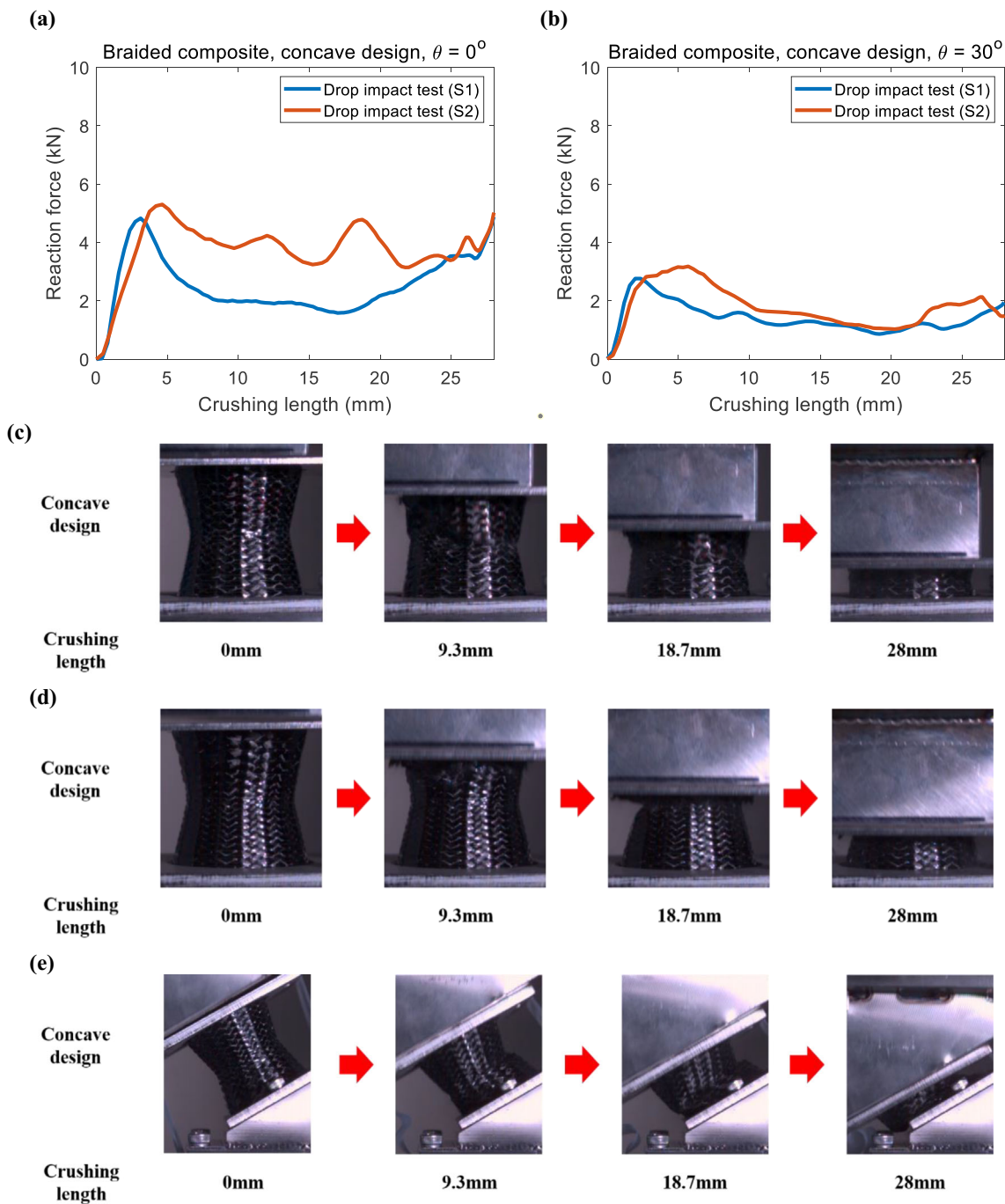


Fig. 9 A braided composite, concave energy absorbing structure under low-velocity impact loading: reaction force-crushing length curve, **a** $\theta = 0^\circ$, **b** $\theta = 30^\circ$; crushing process, **c** $\theta = 0^\circ$ (S1), **d** $\theta = 0^\circ$ (S2), **e** $\theta = 30^\circ$

3.6 Braided Composite Energy Absorbing Structures with Convex Design

A drop impact test was conducted for the convex design. The convex design, like the concave design, features a bent central portion, exhibiting similar structural characteristics. The reaction force-crushing length curve in Fig. 10a and b

confirms early densification for both the axial loading and the combined shear-compression loading. Figure 10c and d illustrates the crushing process based on the load angle. Initial crushing was induced in the weakened central region due to the bending of fibers, and as cracks generated, the load-bearing performance decreased. This resulted in a deterioration of energy absorption performance.

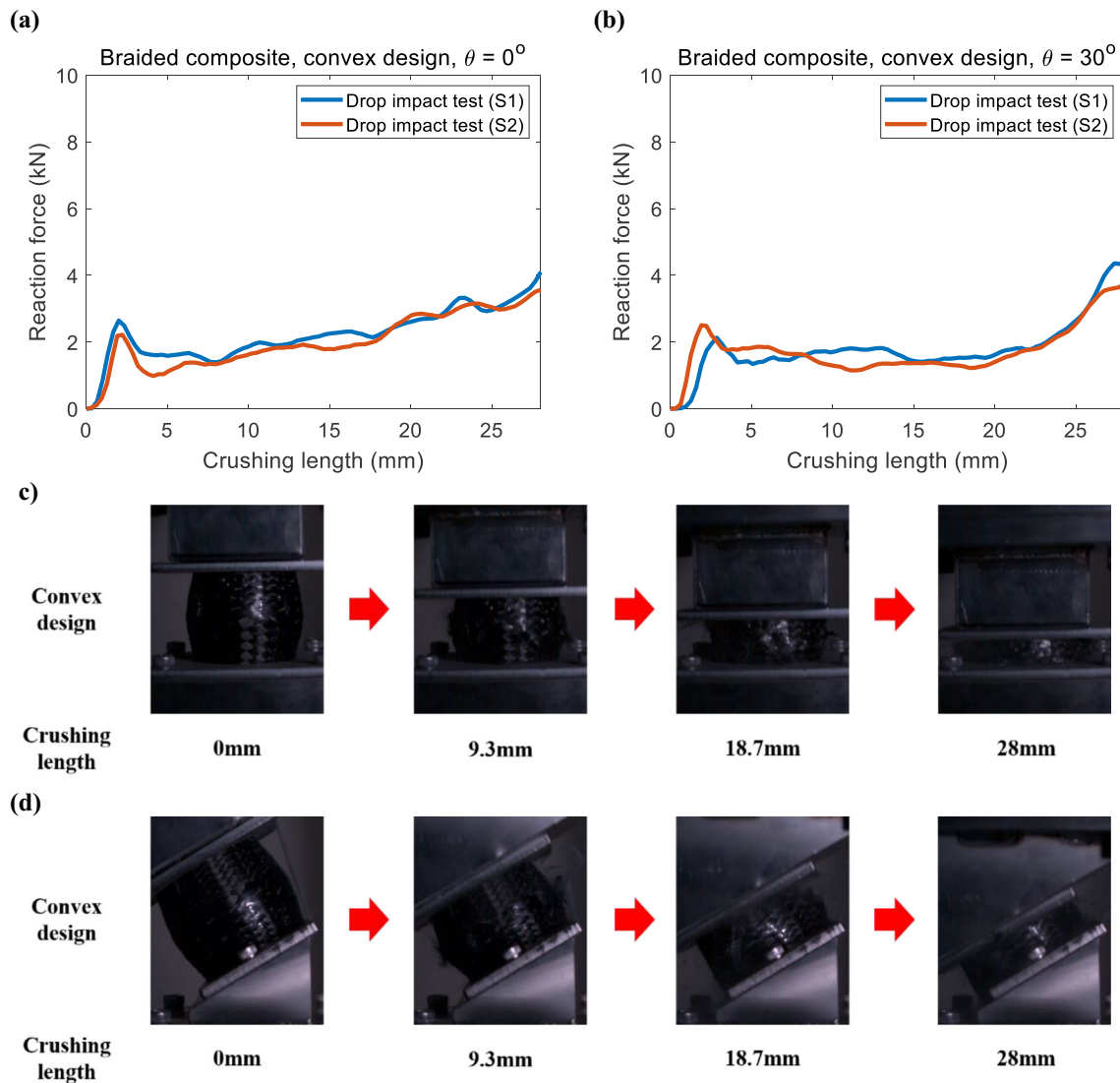


Fig. 10 A braided composite, convex energy absorbing structure under low-velocity impact loading: reaction force-crushing length curve, **a** $\theta = 0^\circ$, **b** $\theta = 30^\circ$; crushing process, **c** $\theta = 0^\circ$, **d** $\theta = 30^\circ$

3.7 Comparative Study

The crashworthiness performance was compared based on geometries and materials. The reaction force-crushing length curves in Figs. 11 and 12 plot the results of the first specimen (S1) test, as presented in preceding section. Additionally, Fig. 13 and Table 3 were formed based on the average values obtained through repeated tests.

In the case of metallic materials, as shown in Fig. 11, it can be observed that the initial crushing load was highest when the straight design was applied. The early stages of crushing did not experience stress concentration from geometric imperfections, resulting in a lowered CFE performance. As indicated in Fig. 13 and Table 3, SEA and E_v performance were superior when the concave design was employed, while

the convex design showed the best CFE performance. The lower SEA and E_v performance in the convex design was attributed to the increased mass and volume for the same end diameter, height, and thickness.

As shown in Fig. 12, the load-bearing performance of the straight design was consistently superior throughout the entire crushing process. This superiority can be attributed to the induction of a progressive crushing mode through shear failure at the end. Although the load-bearing performance experienced a significant decline after the initial crushing at a 30-degree load angle, along with the simultaneous induction of the bending mode, it still demonstrated better load-bearing performance compared to other geometries. As indicated in Fig. 13 and Table 3, it can be noted that, except for the CFE

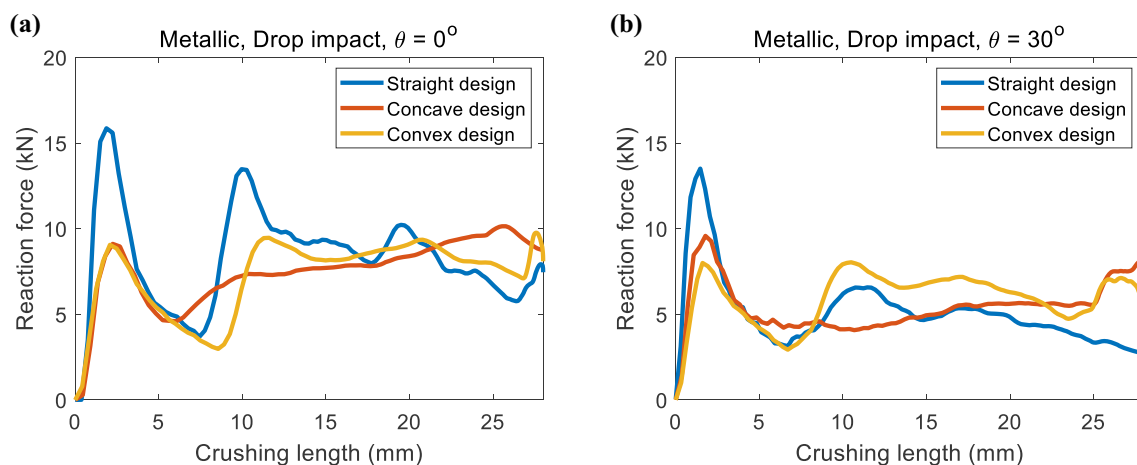


Fig. 11 Reaction force-crushing length curve according to loading conditions and geometry (Metallic material): **a** $\theta = 0^\circ$, **b** $\theta = 30^\circ$

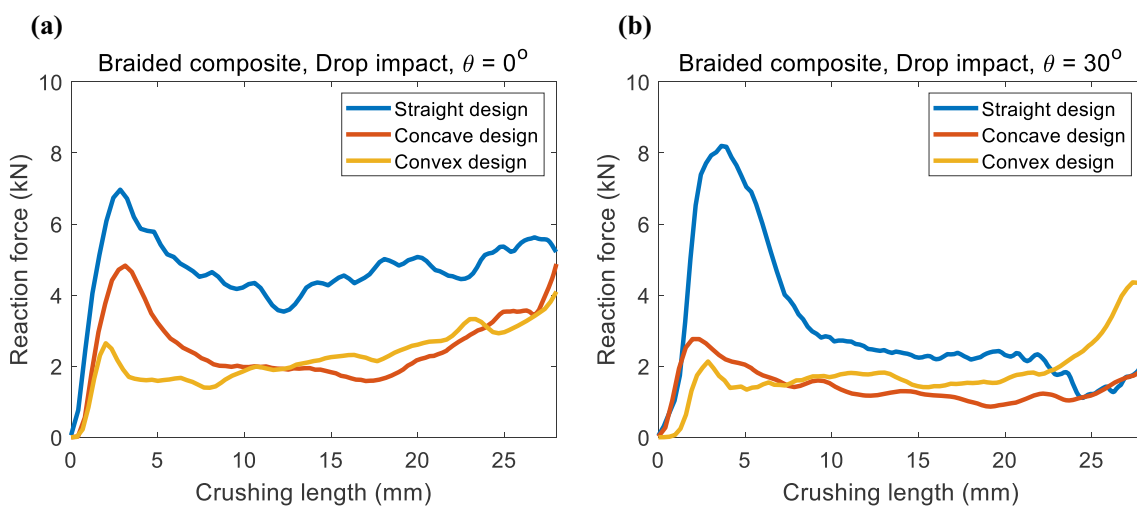


Fig. 12 Reaction force-crushing length curve according to loading conditions and geometry (Braided composite): **a** $\theta = 0^\circ$, **b** $\theta = 30^\circ$

performance at a 30-degree load angle, crashworthiness was most superior when the straight design was applied.

The effects of the constituting materials on the crashworthiness performance of the energy absorbing structure were compared. As indicated by Fig. 13b, the SEA of the braided composite energy absorbing structure is consistently superior. However, referring to Fig. 13c, it can be observed that the energy absorption per volume is consistently superior for metallic energy absorbing structures. Therefore, the selection of materials may vary depending on the weights assigned to SEA and E_v . Depending on the application, both metallic material and braided composite can be effectively utilized as materials for energy absorbing structures.

Additionally, through Fig. 13d, it is evident that the CFE of metallic energy absorbing structures with concave or convex designs is consistently superior. This is because, with the application of concave design and convex design to energy

absorbing structures made from metallic materials, the initial crushing load was reduced due to stress concentration. Moreover, the load-bearing performance in the remaining structural areas was well-maintained, allowing for an even distribution of load across the structure.

As shown in Fig. 13, the effective geometry for harnessing the energy absorption performance of metallic material and braided composite varies due to their different energy absorption mechanisms. For metallic material, it is appropriate to induce initial crushing and evenly distribute the load across the entire structure to maximize plastic deformation through geometric changes like concave design. On the other hand, for braided composite, the damage accumulation in the laminate must be maximized. To achieve this, a straight design that induces initial crushing by shear failure at the ends and promotes a progressive crushing mode may be suitable.

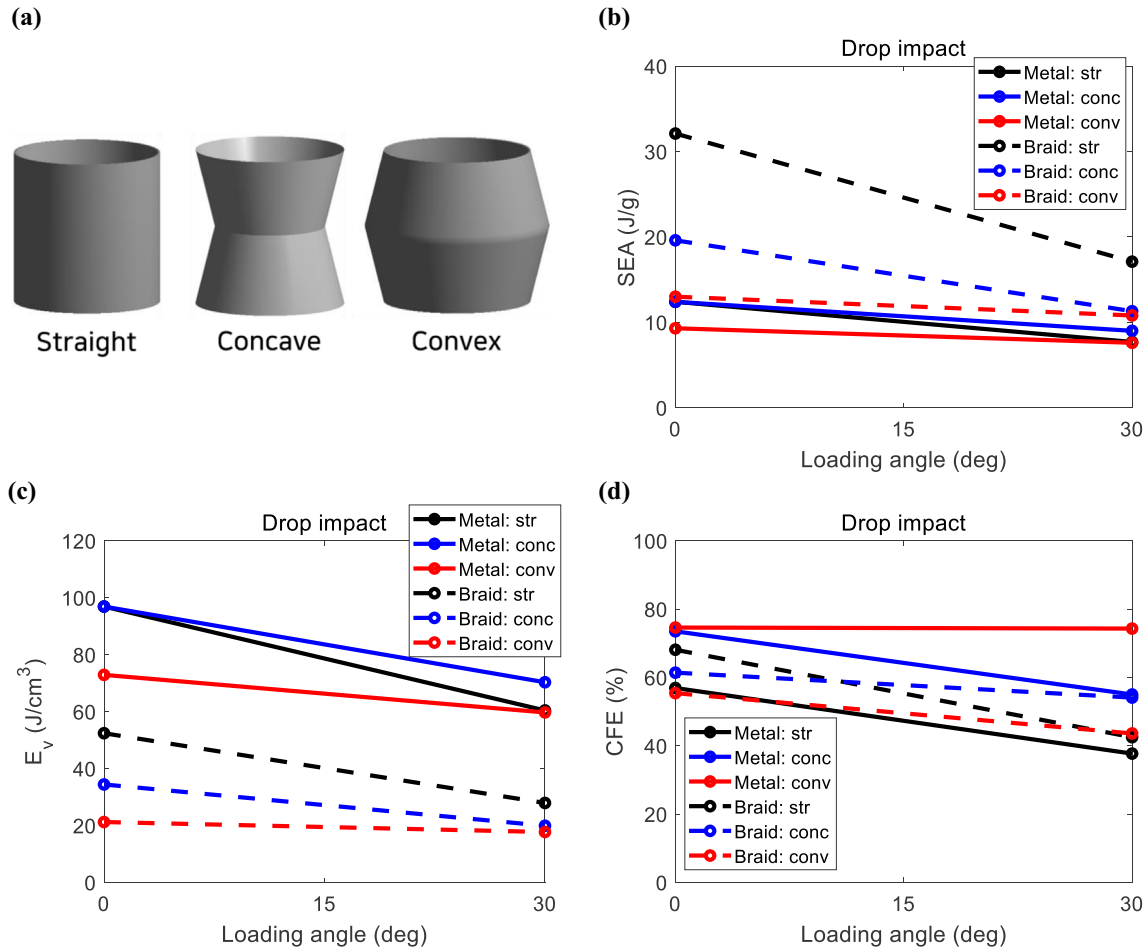


Fig. 13 Comparison between metallic material and braided composite: **a** Geometry, **b** SEA – θ , **c** E_v – θ , **d** CFE – θ . (θ = loading angle). *str = straight, conc = concave, conv = convex, Braid = braided composite

Table 3 Comparison of crashworthiness according to load conditions and geometry: metal vs braided composite

| Geometry | | Loading angle (deg) | SEA (J/g) | CFE (%) | E_v (J/cm ³) |
|-------------------------|----------|---------------------|-----------|---------|----------------------------|
| Metallic material (EGI) | straight | 0 | 12.4 | 56.9 | 96.9 |
| | | 30 | 7.7 | 37.7 | 60.4 |
| | concave | 0 | 12.4 | 73.5 | 96.9 |
| | | 30 | 9.0 | 55.0 | 70.3 |
| | convex | 0 | 9.3 | 74.6 | 72.9 |
| | | 30 | 7.6 | 74.3 | 59.7 |
| Braided composite | straight | 0 | 32.1 | 68.1 | 52.4 |
| | | 30 | 17.1 | 42.5 | 27.9 |
| | concave | 0 | 19.6 | 61.4 | 34.4 |
| | | 30 | 11.3 | 54.1 | 19.9 |
| | convex | 0 | 13.0 | 55.4 | 21.2 |
| | | 30 | 10.8 | 43.6 | 17.7 |

4 Conclusions

In this paper, a study on the design of energy absorbing structures that effectively utilize the energy absorption principles of the material under the combined shear-compression loading was conducted. Metals and braided composites are primarily used in energy absorbing structures, and their energy absorption principles vary depending on the characteristics of the constituent materials. For metal energy absorbing structures, a design that maximizes energy absorption through plastic deformation, leveraging the material's high ductility, is required. The braided composite energy absorbing structure exhibits superior specific stiffness, specific strength, and specific energy absorption performance compared to metals; however, it has lower ductility than metals, leading to predominantly brittle failure. To maximize the performance of the braided composite energy absorbing structure, a geometry that maximizes the accumulation of damage in the laminate should be applied.

To effectively utilize the energy absorption principles of the constituent materials, straight design, concave design, and convex design were analyzed. Additionally, drop impact tests were conducted to validate the structural characteristics. Based on the test results, it is evident that the effectiveness of geometric shapes in enhancing crashworthiness varies according to the energy absorption principles of the constituent materials. Metal energy absorbing structures require geometric designs to maximize plastic deformation, and the application of concave design effectively improves SEA (specific energy absorption) and CFE (crush force efficiency) for the combined shear-compression loading. This improvement is attributed to the structural characteristics of concave design. Convex design exhibits enhanced CFE performance similar to concave design, but with the same end-diameter, height, and thickness, an increase in mass and volume leads to reduced SEA performance. For braided composite energy absorbing structures, utilizing straight design is sufficient to maximize the laminate damage accumulation. By utilizing a straight design, it is possible to induce initial crushing due to shear failure at the ends and promote a progressive crushing mode. When applying concave design or convex design, the strength of the fiber is diminished as the central region takes on a bent shape, leading to a weakening of the load-bearing performance. Additionally, as the load is applied, cracks induced by interaction between adjacent fiber bundles occur, further compromising the load-bearing performance. While SEA performance is consistently superior for braided composite energy absorbing structures, E_v (Energy absorption per unit volume) is consistently better for metallic energy absorbing structures.

In summary, the change in the principles of energy absorption depending on the constituent materials leads to variations

in the geometry that can effectively utilize the material's characteristics. The selection of materials may vary depending on the weights assigned to SEA and E_v , and both metallic material and braided composite can be effectively utilized depending on applications.

Acknowledgements This research was supported by the Challengeable Future Defense Technology Research and Development Program (No.912766601) of Agency for Defense Development in 2023.

Funding Open Access funding enabled and organized by KAIST.

Data availability All data generated or analyzed during this study are included in this published article with appropriated citation.

Declarations

Conflict of interest The authors declare that there is no conflict of interest regarding the publication of this manuscript. Jae-Hung Han is an Associate Editors-in-Chief of IJASS; his status has no bearing on editorial consideration.

Open Access This article is licensed under a Creative Commons Attribution 4.0 International License, which permits use, sharing, adaptation, distribution and reproduction in any medium or format, as long as you give appropriate credit to the original author(s) and the source, provide a link to the Creative Commons licence, and indicate if changes were made. The images or other third party material in this article are included in the article's Creative Commons licence, unless indicated otherwise in a credit line to the material. If material is not included in the article's Creative Commons licence and your intended use is not permitted by statutory regulation or exceeds the permitted use, you will need to obtain permission directly from the copyright holder. To view a copy of this licence, visit <http://creativecommons.org/licenses/by/4.0/>.

References

1. D. C. Fleming and K. E. Jackson. Crashworthy Composite Structures: Aircraft & Vehicle Applications. DEStech Publications, Incorporated, 2021. <https://books.google.co.kr/books?id=phXXzQEACAAJ>.
2. G. Lu and T. Yu. Energy absorption of structures and materials. Elsevier, 2003. <https://www.sciencedirect.com/book/9781855736887/energy-absorption-of-structures-and-materials>.
3. Ma J, Chai S, Chen Y (2022) Geometric design, deformation mode, and energy absorption of patterned thin-walled structures. *Mech Mater* 168:104269. <https://doi.org/10.1016/j.mechmat.2022.104269>
4. Harris J, McShane G (2020) Metallic stacked origami cellular materials: Additive manufacturing, properties, and modelling. *Int J Solids Struct* 185:448–466. <https://doi.org/10.1016/j.ijsolstr.2019.09.007>
5. Zhao H, Abdennadher S (2004) On the strength enhancement under impact loading of square tubes made from rate insensitive metals. *Int J Solids Struct* 41(24–25):6677–6697. <https://doi.org/10.1016/j.ijsolstr.2004.05.039>
6. Marsolek J, Reimerdes H-G (2004) Energy absorption of metallic cylindrical shells with induced non-axisymmetric folding patterns. *Int J Impact Eng* 30(8–9):1209–1223. <https://doi.org/10.1016/j.ijimpeng.2004.06.006>
7. Liu L, Guan Z (2023) Influence of Fillers on the Post-buckling Behavior of the Hat-Stiffened Composite Panels. *Int J Aeronaut*

- Space Sci 24(5):1271–1282. <https://doi.org/10.1007/s42405-023-00607-2>
8. Park IK, Lim JS, Kim SJ (2020) Numerical Study on Energy Absorption of Crashworthy Composite Structure for Helicopters. *KSME* 44(12):947–958. <https://doi.org/10.3795/KSME-A.2020.44.12.947>
 9. Yu Z, Liu X, Wang J, You Q, Fu Y (2021) Shock absorber with inward-folding composite tube and its application in legged landing gear. *Int J Crashworthiness* 26(4):388–403. <https://doi.org/10.1080/13588265.2020.1718463>
 10. Yu Z, Zhou X, Zhou X, Zhang Y, Zhu Q (2020) Crashworthy subfloor structure of civil aircraft via inclined inward-folding composite tubes. *Compos B Eng* 189:1–10. <https://doi.org/10.1016/j.compositesb.2020.107887>
 11. H. Yang and Y. Ren. Stacking design of uniaxial/biaxial braided composite tube under low-velocity impact load. *Mech Adv Mater Struct.* (2023) 1–14. <https://doi.org/10.1080/15376494.2023.2166169>.
 12. Wu Z, Qin S, Zhang P, Pan Z, Hu X, Shi L (2023) Damage evolution in braided composite tubes under axial compression studied by combining infrared thermography and X-ray computed tomography. *Compos Struct* 307:116634. <https://doi.org/10.1016/j.compstruct.2022.116634>
 13. Wu Z, Ding H, Ying Z, Yuan Y, Hu X (2017) Influence of braided fabric on the fracture modes of a composite tube under quasi-static compression. *J Reinf Plast Compos* 36(10):766–779. <https://doi.org/10.1177/0731684417690927>
 14. Gui L, Zhang P, Fan ZJ (2009) Energy absorption properties of braided glass/epoxy tubes subjected to quasi-static axial crushing. *Int J Crashworthiness* 14(1):17–23
 15. M. N. Roslan, M. Y. Yahya, Z. Ahmad and A. Azrin Hani. Energy absorption behaviour of braided basalt composite tube. *Adv Compos Mater.* 27 (5) (2018) 467–481.
 16. Li Y, You Z (2019) Origami concave tubes for energy absorption. *Int J Solids Struct* 169:21–40. <https://doi.org/10.1016/j.ijsolstr.2019.03.026>
 17. Aljibori HSS, Alosfur FKM, Ridha NJ (2018) Effect of crushing speed rate on crashworthiness parameters and energy absorption capability of composite materials. *J Phys Conf Ser* 1032(1):012074. <https://doi.org/10.1088/1742-6596/1032/1/012074>
 18. Ming S, Song Z, Li T, Du K, Zhou C, Wang B (2020) The energy absorption of thin-walled tubes designed by origami approach applied to the ends. *Mater Des* 192:108725. <https://doi.org/10.1016/j.matdes.2020.108725>
 19. Ming S, Song Z, Zhou C, Li T, Du K, Xu S, Wang B (2021) The energy absorption of long origami-ending tubes with geometrical imperfections. *Thin-Walled Struct* 161:107415. <https://doi.org/10.1016/j.tws.2020.107415>
 20. Yang H, Lei H, Lu G, Zhang Z, Li X, Liu Y (2020) Energy absorption and failure pattern of hybrid composite tubes under quasi-static axial compression. *Compos B Eng* 198:108217. <https://doi.org/10.1016/j.compositesb.2020.108217>
 21. Zhu G, Sun G, Liu Q, Li G, Li Q (2017) On crushing characteristics of different configurations of metal-composites hybrid tubes. *Compos Struct* 175:58–69. <https://doi.org/10.1016/j.compstruct.2017.04.072>
 22. Lykacos SS, Kostazos PK, Venetsanos O-V, Manolakos DE (2021) Crashworthiness Performance of Aluminium, GFRP and Hybrid Aluminium/GFRP Circular tubes under quasi-static and dynamic axial loading conditions: a comparative experimental study. *Dynamics* 1(1):22–48. <https://doi.org/10.3390/dynamics1010004>
 23. Hwang Y-H, Han J-H (2024) Energy absorption optimisation of an origami-shaped crash box under axial loading. *Int J Crashworthiness* 29(1):132–141. <https://doi.org/10.1080/13588265.2023.2196909>
 24. Zhou C, Wang B, Ma J, You Z (2016) Dynamic axial crushing of origami crash boxes. *Int J Mech Sci* 118:1–12. <https://doi.org/10.1016/j.ijmecsci.2016.09.001>
 25. Zhou C, Jiang L, Tian K, Bi X, Wang B (2017) Origami crash boxes subjected to dynamic oblique loading. *J Appl Mech* 84(9):1–11. <https://doi.org/10.1115/1.4037160>

Publisher's Note Springer Nature remains neutral with regard to jurisdictional claims in published maps and institutional affiliations.